

# The first 30 years of research on the physical properties of $\alpha$ -U

Edward S. Fisher

Materials Consulting Services, Cedar Knoll Ct., Minnetonka, MN 55305 (USA)

## Abstract

Uranium metal has three allotropic phases in the solid state, with a melting point of 1405 K. The  $\alpha$  phase crystal (0–940 K) has orthorhombic symmetry, which is unique among unalloyed metals, and, because of its dimensional instability as a fuel element in early nuclear reactors, has a nearly unique history as a subject for solid state research. The need to understand its behavior under neutron irradiation sparked a world-wide effort to investigate the anisotropic properties of the crystal and its polycrystalline aggregates. Methods for metal purification and for preparing single crystals were followed by very precise measurements of mechanical and physical properties in general. The unusual scope of the research was enhanced by the discovery of a second-order phase transition at 43 K and speculations regarding magnetic structures and superconductivity of uranium and the other 5f elements. In this review some of the early research beginning in 1948 and the low temperature and high pressure research that followed up to 1978 are described. This precedes the surprising discovery of the charge-density-wave structures that emerged from the lattice dynamic studies and neutron elastic scattering in 1979 and 1980.

## 1. Introduction

This review is a brief summary of research on the metallurgical properties of  $\alpha$ -U that began with the establishment of the USAEC National Laboratories, the Harwell Laboratory in England and the Saclay Laboratory in France, beginning about 1948. Because of the unique crystal structure with orthorhombic symmetry (Fig. 1) that was discovered by Jacob and Warren

[1], there was not only a world-wide interest in probing the properties of uranium in the elevated temperature regime that was pertinent to reactor fuel applications, but also a casual academic interest using newly developed cryogenic tools to explore possibilities of magnetic structures and superconductivity. The latter investigations led to ambiguities and uncertainties regarding superconductivity, specific heat parameters and electron transport properties in polycrystalline samples, that were explained to some degree by the discovery of phase transitions at 43 K, 37 K and 22.5 K and the ongoing X-ray and neutron diffraction studies of these charge-density-wave (CDW) phase transitions [2]. The intent here is to provide the highlights that occurred during 1948–1978, the pre-CDW era.

## 2. Summary of research

### 2.1. Preparation of single crystals

The primary objective of several of the AEC National Laboratories in 1948 was the development of both thermal and fast breeder reactors for power production. As in the Pu producing reactors, the initial fuel was to be made from a good grade of unalloyed uranium metal. Like the Hanford reactors, the fuel elements would encounter the dimensional instability problems produced by neutron irradiation damage. Unlike the Pu producers, the fuel would be held at high tem-

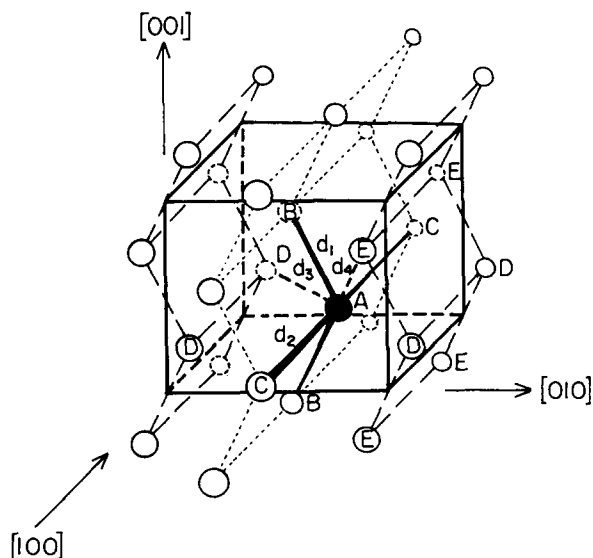


Fig. 1. Crystal structure of  $\alpha$ -U.

peratures for extraction of the heat energy and would remain in the reactor as long as feasible for efficient power production. It thus appeared mandatory to understand the mechanism of the dimensional instability and its dependence on metallurgical parameters, such as grain size, and preferred orientation, or texture, as shown in Fig. 2. This required that the anisotropic physical and mechanical properties of the orthorhombic crystal be known from direct measurements on single-crystal samples.

The efforts to produce  $\alpha$ -U single crystal began in early 1948 at Argonne National Laboratory, Knolls Atomic Power, Harwell and Saclay. Because of the two first-order phase transformations that occur between the melting point (1406 K) and the  $\alpha$  phase, at 933 K, the initial plans and efforts involved essentially two different techniques, (1) a modified Bridgman method [3] and (2) a strain-anneal grain growth within the  $\alpha$  phase [3]. The former produced long  $\alpha$  grains that were, in turn, subgrained into mosaic blocks that varied in crystal orientation by as much as  $10^\circ$  rotation about a zone axis. The strain-anneal method could not be successfully applied to  $\alpha$ -U because of the multiplicity of recrystallization nuclei produced by deformation twinning [3]. However, through a comprehensive study of grain growth as a function of metal purity, the team of metallurgists under Frank Foote at Argonne National Laboratory developed a procedure for growing cylindrical single crystals of  $\alpha$ -U by the mechanism of grain coarsening, which did not involve recrystallization nuclei [4]. The optimum single-crystal dimensions were about 6 mm in diameter and 1 cm long (Fig. 3). The X-ray

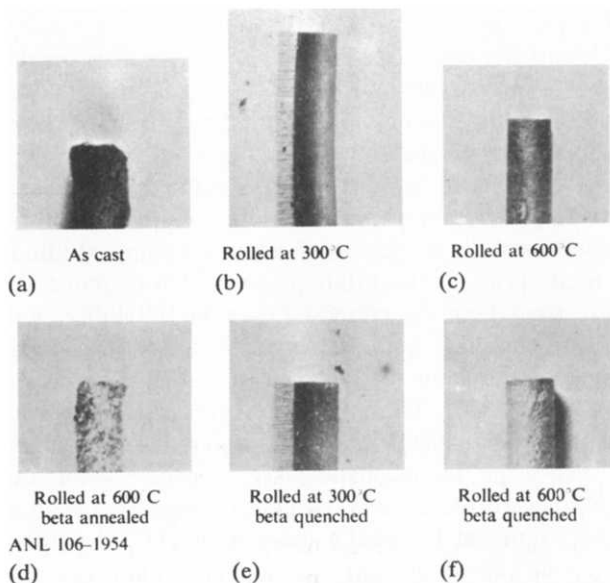


Fig. 2. Relative appearance of various  $\alpha$ -U samples after irradiation to 0.1% burn-up.

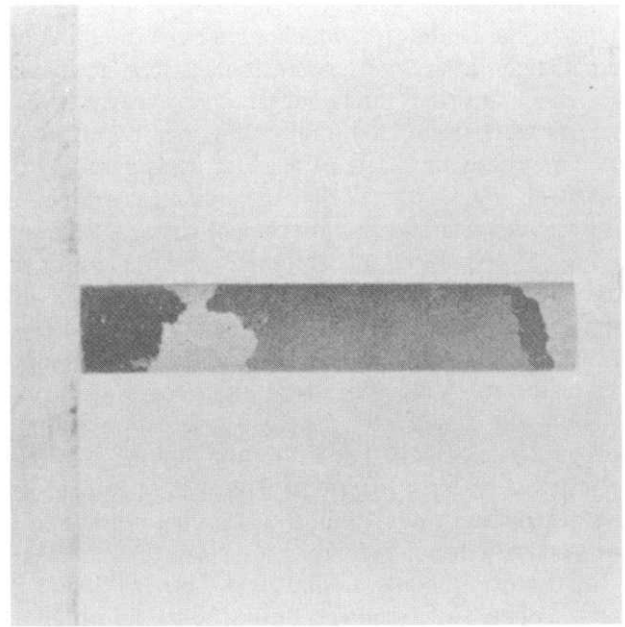


Fig. 3. Sample containing cylindrical single crystal obtained by grain coarsening [4].

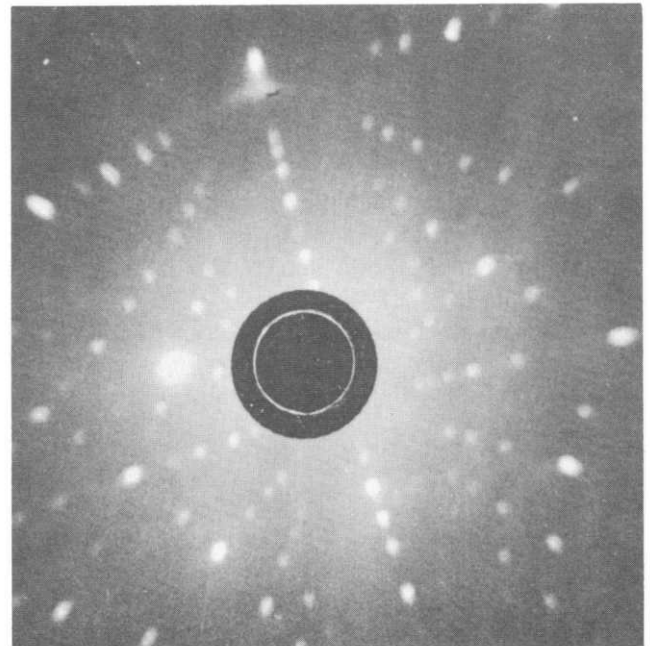


Fig. 4. Typical X-ray back-reflection Laue spots from single crystals obtained by coarsening [4].

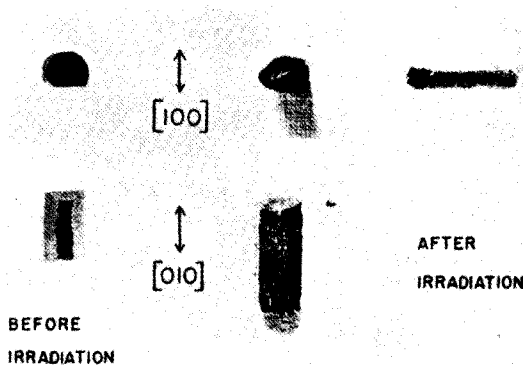
diffraction Laue patterns reveal no lineage or mosaic structural imperfections (Fig. 4).

## 2.2. Irradiation growth

Prior to the availability of the near-perfect single crystals it was generally assumed that the mechanism of growth by neutron irradiation was related directly to the mechanism of elongation during thermal cycling

of polycrystalline aggregates [5]. The results of the single-crystal studies [6], which were performed almost immediately after the crystals were first available, showed clearly the fundamental differences between the two mechanisms: thermal cycling has no effect on the dimensions or shape of a good, as opposed to an imperfect, single crystal of  $\alpha$ -U, whereas irradiation produces very significant dimensional changes as shown in Fig. 5. Experiments performed simultaneously at Argonne and Knolls showed that after irradiation with the sample at 350 K, producing 0.1% fission burn-up of the 235 isotope, the [010] crystal increases in length by a factor of 1.5, whereas the [100] direction decreases in about the same ratio. The [001] direction exhibits no significant growth. Thus the pronounced growth of polycrystals with a [010] fiber texture is related to the crystal structure rather than the grain boundary effects involved in thermal cycling.

In later experiments, Loomis and Gerber [7] showed that the dimensional changes during neutron irradiation in the [010] and [100] directions are markedly enhanced when the crystals are at temperatures below 50 K, with very large changes occurring between 20 K and 40 K (Fig. 6). The growth coefficients for the near-perfect crystals are about twice those for the pseudocrystals, apparently reflecting the smaller number of defects present before irradiation. Adopting the growth models proposed by Buckley [8] and Hudson [9], the defects causing the growth in [010] and shrinkage in [100] consist of clusters of interstitials on (010) planes and vacancy clusters on (100) planes. The Loomis and Gerber data imply that the point defect mobility is markedly enhanced in the CDW structures below 43 K and becomes very mobile at the lock-in transition below 22 K. These conclusions are consistent with the quenched-in electrical resistivity studies of Jousset [10].



ANL 106-1954

Fig. 5. Single crystal before and after irradiation in reactor to 0.1% burn-up [6].

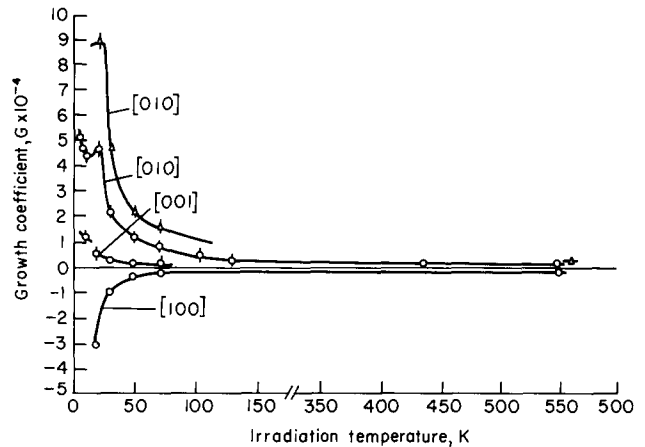


Fig. 6. Effect of irradiation temperature on the growth coefficient of single crystals, pseudocrystals and polycrystals [7].  $\Delta$ , single crystal [010];  $\circ$ , pseudo single crystal [010];  $\diamond$ , pseudo single crystal [001];  $\blacksquare$ , pseudo single crystal [100];  $\bullet$ , polycrystal.

TABLE 1. Weighted mean values for the stiffness moduli in  $\alpha$ -U at 295 K

Modulus	Value ( $\times 10^{12}$ dyn $\text{cm}^{-2}$ )
$C_{11}$	2.1474
$C_{22}$	1.9857
$C_{33}$	2.6711
$C_{44}$	1.2444
$C_{55}$	0.7342
$C_{66}$	0.7433
$C_{12}$	0.4646
$C_{13}$	0.2183
$C_{23}$	1.0755

From Fisher and McSkimin [11]. All values  $\pm 0.14\%$ .

### 2.3. Elastic modulus studies

One of the objectives of this survey is to explain the many disagreements and inconsistencies in the physical property measurements of  $\alpha$ -U that are brought about by anisotropy in the single-crystal properties and preferred orientation in most polycrystalline uranium samples. A prime example is the anisotropy of the elastic properties of the single crystal, namely Young's modulus  $E$ , as it varies in the (100) plane, which contains the nearest-neighbor direction at  $27^\circ$  to the [001] direction. Young's modulus increases by 25% from the  $C_0$  axis to a maximum value at  $37^\circ$  to [001] and then decreases by 47% at [010]. These  $E$  values are calculated from the nine single-crystal stiffness moduli  $C_{ij}$  as determined by measuring the acoustic wave velocities using the high precision ultrasonic wave phase comparison method of McSkimin at the Bell Laboratories [11]. Details of the single-crystal samples, the experimental procedure and the results are given in ref. 11. The values of the nine stiffness moduli for  $\alpha$ -U are given in Table 1.

#### 2.4. Elastic moduli at cryogenic temperatures

The single-crystal elastic moduli studies have been extended from ambient temperatures to 923 K [12] and down to 2.5 K [12–15]. The first indications of anomalies in the elastic properties at  $T < 300$  K were found in the  $C_{11}$  modulus, that represents the ratio of stress to elastic strain,  $T_x/e_x$  in the [100] direction noted in Fig. 1. Whereas the  $C_{22}$ ,  $C_{33}$ ,  $C_{44}$ ,  $C_{55}$ , and  $C_{66}$  moduli exhibited the normal negative and nearly linear temperature derivatives between 573 K and 77 K,  $C_{11}$  has its maximum value at 256 K and a sharply increasing positive derivative on approaching 77 K.

On cooling below 50 K,  $C_{11}$  decreases almost abruptly to 43 K, where the ultrasonic wave energy is completely attenuated by what we now know as the atomic displacements, primarily in the [100] direction, involved in the transition to a CDW phase. The extremely large adjustments in  $C_{11}$  are plotted in Fig. 7. From its maximum value of 215 GPa at 256 K it decreases to well below 100 GPa between 43 K and 37 K, and then increases sharply on cooling to 114 GPa at 0 K. On warming, however,  $C_{11}$  decreases well below the cooling curve to a sharp minimum value at 22 K, where it then increases slightly before joining the cooling curve. The above data, together with very detailed monitoring of  $C_{33}$ ,  $C_{44}$ , and  $C_{66}$  vs. temperature, described in ref. 15, identify 22 K and 38 K, as well as 43 K, as transition temperatures at which temperature derivatives change abruptly. This behavior is not typical of first-order phase transitions.

#### 2.5. Thermal expansion in $\alpha$ -U

Measurements of the three thermal expansion coefficients have played a major role in uncovering the mysterious behavior of the  $\alpha$ -U crystal. The first indications of anomalous properties were noted in a classified 1944 document [16], where X-ray diffraction measurements of the lattice constants at 298 K, 573 K and 923 K detected a negative expansion coefficient in the  $b_0$  lattice constant between 298 K and 573 K. Subsequent X-ray diffraction studies on polycrystals by Bridge *et al.* [17] confirm the negative thermal expansion coefficient for  $b_0$  at  $T > 298$  K, but show that the contraction is enhanced with  $T$  all the way to the  $\alpha$ - $\beta$  transformation. The Bridge *et al.* data also indicate a minimum value for the  $a_0$  parameter between 20 K and 63 K, but no anomalies in  $b_0$  or  $c_0$ . The later work by Barrett *et al.* [18], shown in Fig. 8, used both X-ray and neutron diffraction on single-crystal samples and establish that both the  $a_0$  and  $b_0$  parameters exhibit anomalous minima at 43 K, whereas the decrease in the  $c_0$  parameter with decreasing temperature is markedly enhanced between 43 K and 20 K. These X-ray results were confirmed and amplified by Steinitz *et al.* [19] using a supersensitive strain gauge. These data

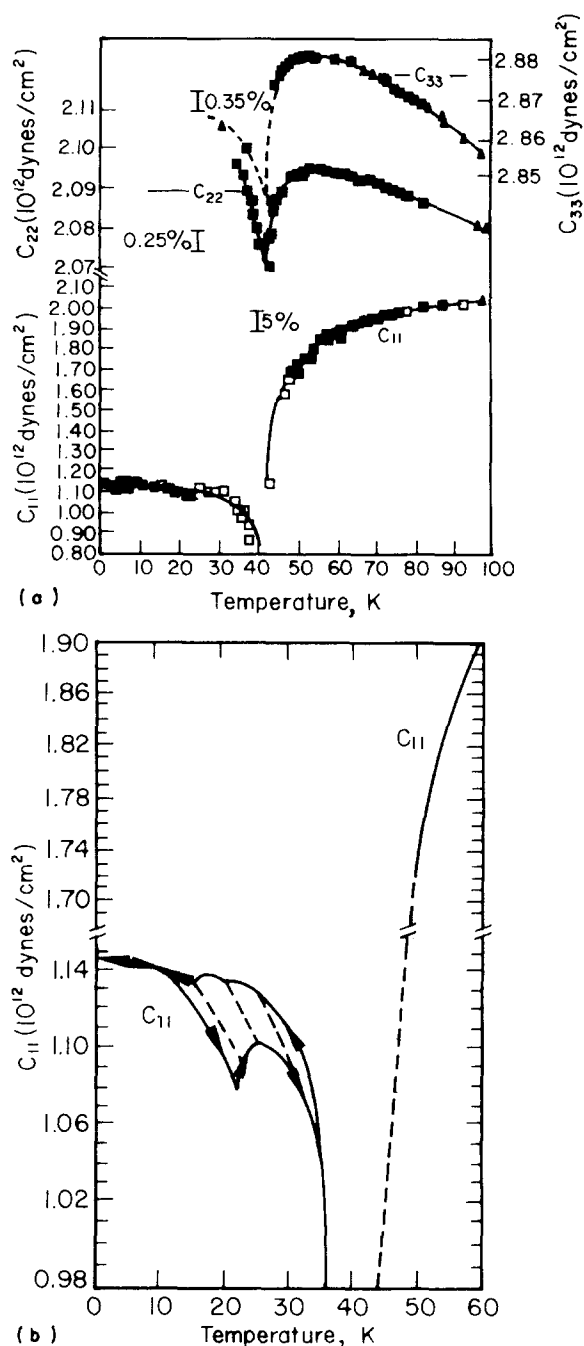


Fig. 7. (a)  $C_{11}$ ,  $C_{22}$  and  $C_{33}$  vs. temperature at the 43 K CDW transition [14]. (b) Details of hysteresis in  $C_{11}$  at the 22 K transition [15].

indicate that, whereas the 43 K transition does not involve an abrupt shift in any of the lattice constants, the anomalies at 38 K and 22 K indicated by the elastic modulus data are first-order transitions involving abrupt shifts in all three lattice constants.

The work of Barrett *et al.* [18] also showed that the  $y$  positional parameter, describing the coordinates along the  $Y$  axis of the four atoms per unit cell, is not discontinuous at 43 K but  $dY/dT$  does change abruptly

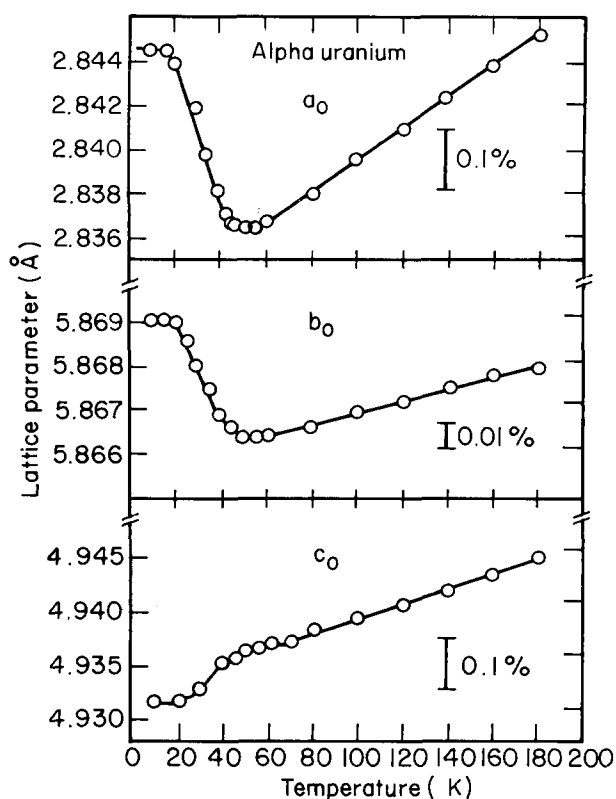


Fig. 8. X-ray diffraction angles  $\theta$  and corresponding lattice constant changes during slow warming from 4 K [18].

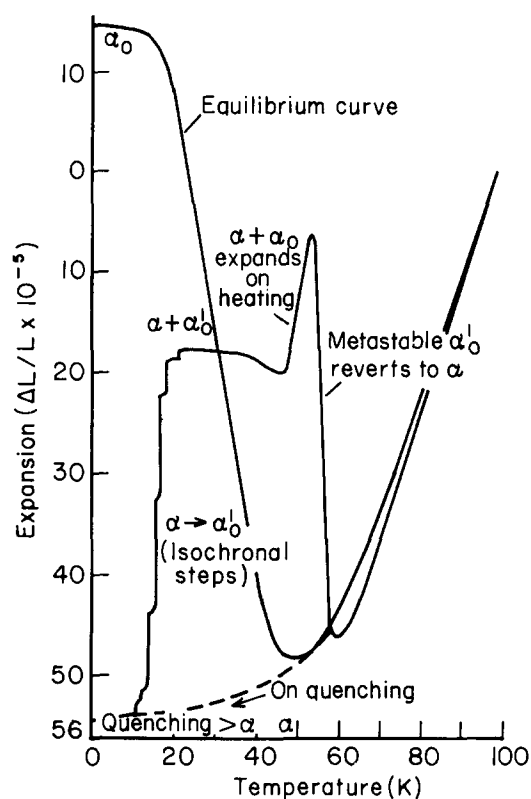


Fig. 9. Thermal expansion of  $\alpha$ -U polycrystal subjected to various heat treatments [22].

from a positive to a negative sign. They also found no change in space group symmetry at  $T=43$  K. These conclusions were confirmed by Lander and Mueller [20] in the first comprehensive neutron diffraction study of  $\alpha$ -U. They also found that the principal neutron intensities increased to peak values at 40 K and remained at high levels at  $T < 40$  K. These increased intensities were ascribed to changes in the extinction parameter that are brought on by the introduction of crystal imperfections at 43 K, which disappear on warming above 43 K. These neutron diffraction experiments and the elastic modulus anomalies were the bases for the inelastic and elastic scattering experiments at Oak Ridge National Laboratory [21] and the discovery of the CDW at  $T < 43$  K.

It is important to note that the above-described anisotropy in thermal expansion is typical only of single crystals and that the inhibition of free expansion or contraction at grain boundaries in a polycrystal is largely responsible for the many differences reported in measured physical properties. These constraints were evidently responsible for the complete suppression of the CDW phase transitions by rapid quenching from above 43 K and 4 K and different non-equilibrium mixtures of CDW and  $\alpha$ -U phases during warming above 10 K, as is shown in Fig. 9, by Hough *et al.* [22].

## 2.6. Heat capacity measurements

The many different measurements of heat capacity at  $T < 300$  K are prime examples of the effects of the constraints on thermal expansion within polycrystalline samples. The measurements performed on polycrystals were in most cases free of anomalies in the 43 K temperature range [23]. Small anomalies were noted only by careful searching [24, 25]. Crangle and Temporal have, however, shown that very clear anomalies can be detected by use of pseudocrystals grown by the modified Bridgeman methods [24]. The transition at 37 K produced a very sharp peak in  $C_p$  on heating and a smaller peak during cooling, whereas the transitions at 22 K and 43 K produced only small rounded anomalies.

The constraints on the CDW transitions appear to have a significant effect on the electronic specific heat coefficient  $\gamma_e$  as determined by  $C_p/T$  vs.  $T^2$  plots at  $T < 10$  K. Table 2 is a listing of 16 different determinations of  $\gamma_e$  of which only two are for single-crystal samples. The  $\gamma_e$  values for the Crangle and Temporal [24] pseudocrystal and for the Bader *et al.* [29] near-perfect crystal are identical at  $9.14 \text{ mJ mol}^{-1} \text{ K}^{-2}$ , whereas the other 14 values vary from 9.46 to  $12.1 \text{ mJ mol}^{-1} \text{ K}^{-2}$ . The value of  $12.2 \text{ mJ mol}^{-1} \text{ K}^{-2}$  reported by Ho *et al.* [28] for a polycrystal at 10 kbar hydrostatic pressure is presumably that for the  $\alpha$  phase without the CDW transitions, as discussed below.

TABLE 2. Values of the electronic specific heat coefficient  $\gamma_e$  and Debye temperature  $H$  for  $\alpha$ -U reported by different investigators

Investigators	$\gamma_e$ (mJ (mol <sup>-1</sup> K <sup>-2</sup> ))	Debye $H$ (K)	Temperature range (K)
Gordon <i>et al.</i> [26]	10.12	182.6	1–4
Ho <i>et al.</i> [28]	10.03	207	
Flotow and Osborne [27]	9.88	218	1–4
1 bar pressure, U10 material	10.3		0.3–6
10 kbar, U10 material	12.2		
Crangle and Temporal [24], U10 material	10.00	195	2–10
Pseudo crystal	9.46	203	
	9.14	210	
Bader <i>et al.</i> [29]	9.59		0.1–0.25
	9.86		
U10 material	9.82		
U10 material	9.90		
Single crystal	9.14		
Smith and Wolcott [30]	10.9	200	
Goodman and Schoenberg [31]	10.6	206	
Dempsey <i>et al.</i> [32]	12.1		

### 2.7. Electrical resistivity and Hall effect

Transport property measurements on  $\alpha$ -U have received considerable attention, beginning with thermal conductivity measurements motivated to provide technical data for cooling the uranium fuel elements in the Pu production reactors. A comprehensive review of the early data is given by Holden [33]. Rosenberg [34] noted small inflections in thermal conductivity *vs.* temperature at 60 K, that he attributed to the transition from electronic to lattice conductivity on heating. However, such small inflections between 50 and 60 K are also typical of several electrical conductivity measurements in polycrystals [35, 36], whereas other data exhibit either no significant inflections or inflections associated with the 37 K transition. These variable results are as expected for the variations in constraints on the CDW transitions in polycrystals. The only study on pseudocrystal samples [37] found small inflections at both 42 K and 37 K. They also found significant differences between heating and cooling through the 22 K transition. This apparent hysteresis is consistent with what is found in the  $C_{11}$  elastic modulus data (Fig. 7). In both cases the differences are independent of the rates of cooling or heating, which is not typical of first-order hysteresis. There is, however, a study of quenched-in resistivity by Jousset [10] where defect migration appears to be involved. Figure 10 shows Jousset's results for pulse annealing of four different pseudocrystals after quenching in liquid helium from 77 K. All the quenched-in resistivity (about 0.15  $\mu\Omega$  cm) disappears after pulse annealing to 18 K, but reappears after quenching back

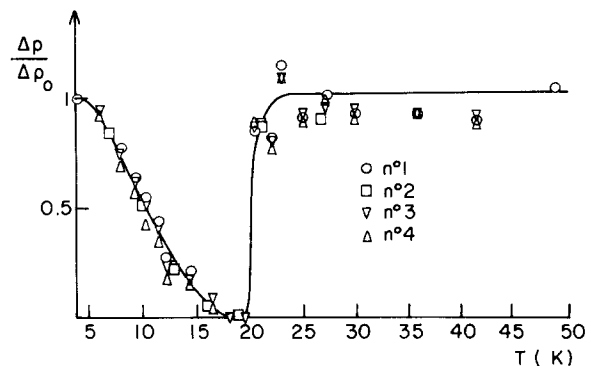


Fig. 10. Annealing out of electrical resistivity quenched in from 77 K to 4 K in four different pseudocrystals.

to 4 K from any temperature above 23 K. With our present knowledge of multiple CDW domains in  $\alpha$ -U at  $T < 22$  K, due to Chen and Lander [38], Jousset's results apparently reflect the quenching in of the incommensurate CDW domains, that are the dominant CDW state above 23 K. The gradual decrease in resistivity after pulse annealing reflects the growth of the equilibrium non-commensurate CDW domains at  $T < 18$  K.

### 2.8. Hall effect

Of all the physical property measurements, the Hall effect data for  $\alpha$ -U are alone in providing some qualitative relation between the CDW atom displacements and the electronic structural changes at the Fermi surface. The data plots by Berlincourt [39] and by

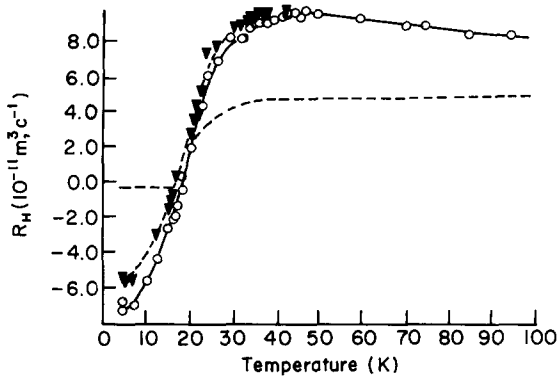


Fig. 11. Hall coefficient as a function of temperature and magnetic field to 1.8 T in pseudocrystals, determined by Cornelius and Smith [40]. ---, data for polycrystal obtained by Berlincourt [39].

Cornelius and Smith [40] are shown in Fig. 11. For Berlincourt's polycrystal there was a rapid and abrupt increase in  $R_H$  from 20 K to 40 K. The pseudocrystal sample of Cornelius and Smith exhibits a much greater change, increasing from a large negative  $R_H$  at 4 K to a maximum positive value at 40 K, with  $R=0$  at approximately 20 K. This change is similar to that observed in the transition metal dichalcogenides where the algebraic sign change suggests a disruption of the Fermi surface topology so as to produce a transfer from hole to electron charge carriers. In later experiments [41] it is shown that the application of only 1.4 kbar of hydrostatic pressure is sufficient to suppress the strong temperature dependence of  $R_H$ . This behavior is in accord with the relatively sharp suppression of the CDW transition temperatures with increasing pressure, as is discussed below.

### 2.9. Superconductivity vs. charge-density-wave transitions

There have been many magnetic measurements to detect superconductivity in  $\alpha$ -U, starting with  $T_c < 0.98$  K by Shoenberg [42]. Since then all report broad transitions for polycrystalline samples, with  $T_c$  as high as 1.3 K at zero hydrostatic pressure, and a few indicating that  $\alpha$ -U is not a bulk superconductor. In 1966, however, there were two critical experiments that established (a) that  $\alpha$ -U is a bulk superconductor in an atmosphere of 10 kbar hydrostatic pressure [28], with  $T_c = 2.0$  K, and (b) good single crystals of  $\alpha$ -U produce a relatively sharp transition [43] even with magnetic measurements, but with a small tail starting at 0.3 K. Nevertheless, the absence of superconductivity in calorimetric investigations led to several proposals that filaments of superconducting retained  $\beta$ -U or impurity phases or filaments of strained  $\alpha$ -U, representing  $\alpha$ -U under high pressure, were responsible for the magnetically detected superconductivity. It was not until the calorimetric

studies by Bader *et al.* [29] that bulk superconductivity at zero pressure was established, with broad transition starting at 0.80 K in polycrystals and a relatively sharp transition beginning at 0.2 K for a good single crystal. It was estimated that  $T_c$  for full superconductivity in the crystal was less than 0.1 K.

Our understanding of why  $T_c$  is so dependent on the metallurgical history of polycrystals did not come about until it was noted that the unusually large  $dT_c/dP$  was related to the phases in the sample at  $T < 43$  K. This revelation emerged from a combination of essentially three investigations reported during the short period of 1970 to 1973. The Fisher and Dever study [44] of the pressure dependence of the transition from the  $\alpha$  phase at 43 K at zero pressure established that  $T_{\alpha}$  decreased linearly with increasing hydrostatic pressure from 0 to 4 kbar, with  $dT_{\alpha}/dP = -3.4$  K kbar $^{-1}$ . The Steinitz *et al.* [19] strain gauge thermal expansion data established that the anomalies at 22.5 K and 37 K noted by Fisher and Dever [15] are indeed phase transitions. The measurements of the superconducting  $T_c$  in pseudocrystals to hydrostatic pressures of 24 kbar [45] established that the increase in  $T_c$  from 0 to 12 kbar actually occurred in three steps, with a large linear increase from 0 to 6 kbar, a nearly constant  $T_c = 2.1$  K between 6 and 8 kbar and a small increase to  $T_c = 2.4$  K at 12 kbar. The combination of  $dT_c/dP$  with  $dT_{\alpha}/dP$  proposed by Smith and Fisher [45] is shown in Fig. 12, where we define the phase boundaries at  $P = 0$  kbar as  $T_{\alpha_1} = 43$  K,  $T_{\alpha_2} = 37$  K and  $T_{\alpha_3} = 22.5$  K. This summation assumes that the  $T_{\alpha}$  vs.  $P$  boundary lines are linear with  $dT_{\alpha_1}/dP = -3.4$  K kbar $^{-1}$ . The first big increase

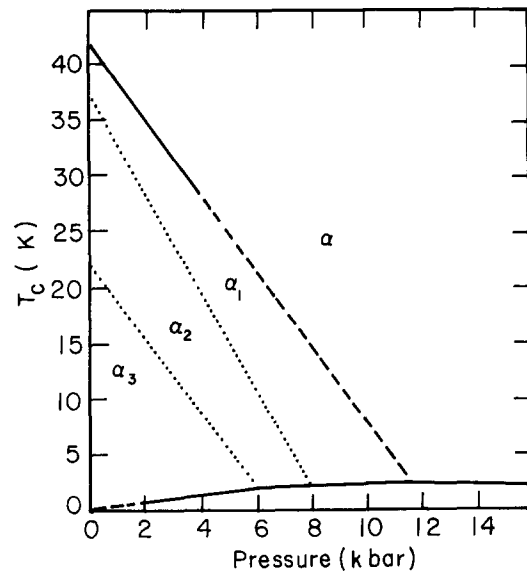


Fig. 12. Proposed phase diagram for low temperature  $\alpha$ -U, relating CDW phase boundaries to stages in the increase in superconducting  $T_c$  with hydrostatic pressure [45].

in  $T_c$  with  $P$  is identified as the destruction of the  $\alpha_3$  phase and  $dT_{\alpha_3}/dP = -3.1 \text{ K kbar}^{-1}$ . This value is very close to the estimate of  $dT_{\alpha_3}/dP = -3.3 \text{ K kbar}^{-1}$  as derived from the Clausius–Clapeyron equation using the latent heat of the  $\alpha_2$  to  $\alpha_3$  transition given by the data of Crangle and Temporal [24] and the relative volume change at the transition given by Steinitz *et al.* [19].

Thanks to the innovative diffraction studies of Smith *et al.* [21] and the surprising direct observations of the CDW phases in single crystal [2] we now know considerably more about the differences between  $\alpha$ ,  $\alpha_1$ ,  $\alpha_2$ , and  $\alpha_3$  and look forward to the ultimate understanding of the effects of these phase changes in terms of the electron energy band structure and Fermi surface topology.

### Acknowledgments

The author is indebted to Pamela Dalman, Elissa Nicholson, Mel Mueller and the Graphic Arts Division at Argonne National Laboratory.

### References

- 1 C.W. Jacob and B.E. Warren, *J. Am. Chem. Soc.*, **59** (1937) 2588.
- 2 G.H. Lander, *Endeavour, New Ser.*, **14** (1990) 179.
- 3 R.W. Cahn, *Acta Metall.*, **1** (1953) 176.
- 4 E.S. Fisher, *Metall. Trans. AIME*, **209** (1957) 882.
- 5 J.E. Burke, J.P. Howe and C.E. Lacey, *USAEC TID Rep.* **74**, 1951.
- 6 S.H. Paine and J.H. Kittel, Irradiation effects in Uranium and its alloys, *1st Genova Conf. on Peaceful Uses of Atomic Energy*, 1955, Paper p/74.5.
- 7 B.A. Loomis and S.B. Gerber, *Philos. Mag.*, **18** (1968) 539.
- 8 S.N. Buckley, *UKAEA Rep. AERE-R5262*, 1966.
- 9 B. Hudson, *Philos. Mag.* **10** (1964) 949.
- 10 J.C. Jousset, *Acta Metall.*, **14** (1964) 193.
- 11 E.S. Fisher and H.J. McSkimin, *J. Appl. Phys.*, **29** (1958) 1473.
- 12 E.S. Fisher, *J. Nucl. Mater.*, **18** (1966) 39.
- 13 H.J. McSkimin and E.S. Fisher, *J. Appl. Phys.*, **31** (1960) 1627.
- 14 E.S. Fisher and H.J. McSkimin, *Phys. Rev.*, **124** (1961) 67.
- 15 E.S. Fisher and D. Dever, *Phys. Rev.*, **170** (1968) 607.
- 16 J.C. Bell, E. Barody, C.M. Schwartz and D.A. Vaughn, *Battelle Memorial, Institute Rep. CT 2002*, 1944, p. 194.
- 17 J.R. Bridge, C.M. Schwartz and D.A. Vaughn, *Metall. Trans. AIME*, **206** (1956) 1282.
- 18 C.S. Barrett, M.H. Mueller and A.R. Hitterman, *Phys. Rev.*, **129** (1963) 625.
- 19 M. Steinitz, C.E. Burleson and J.A. Marcus, *J. Appl. Phys.*, **41** (1970) 5037.
- 20 G.H. Lander and M.H. Mueller, *Acta Crystallogr.*, **26** (1970) 129.
- 21 H.G. Smith, N. Wakabayashi, W.P. Crummett, R.M. Nicklow, G.H. Lander and E.S. Fisher, *Phys. Rev. Lett.*, **44** (1980) 1612.
- 22 A. Hough, J.A.C. Marples, M.J. Mortimer and J.A. Lee, *Phys. Lett.*, **A 27** (1968) 222.
- 23 H. E. Flotow and H. Lohr, *J. Phys. Chem.*, **64** (1960) 904.
- 24 J. Crangle and J. Temporal, *J. Phys. F*, **3** (1973) 1097.
- 25 J.A. Lee, P.W. Sutcliffe and K. Mendelson, *Phys. Lett. A*, **30** (1969) 106.
- 26 J.E. Gordon, H. Montgomery, R.J. Noer, G.R. Pickett and R. Tobon, *Phys. Rev.*, **152** (1966) 432.
- 27 H. E. Flotow and D.W. Osborne, *Phys. Rev.*, **151** (1966) 564.
- 28 J.C. Ho, N.E. Phillips and T.F. Smith, *Phys. Rev. Lett.*, **17** (1966) 694.
- 29 S.D. Bader, N.E. Phillips and E.S. Fisher, *Phys. Rev. B*, **12** (1975) 4929.
- 30 P.L. Smith and N.M. Wolcott, *Proc. Low Temperature Physics Conf., Paris, 1955, Supplement au Bulletin de l'Institut du Froid*, 1955, p. 283.
- 31 B.B. Goodman and D. Shoenberg, *Nature (London)*, **165** (1950) 442.
- 32 C.W. Dempsey, J.E. Gordon and R.H. Romer, *Phys. Rev. Lett.*, **11** (1963) 547.
- 33 A.N. Holden, *Physical Metallurgy of Uranium*, Addison-Wesley, Reading, MA, 1958.
- 34 H.M. Rosenberg, *Philos. Trans. R. Soc. London, Ser. A*, **247** (1955) 441.
- 35 S. Arajs and R.V. Colvin, *J. Less-Common Met.*, **7** (1964) 54.
- 36 G.T. Meaden and J.A. Lee, *Cryogenics*, **1** (1960) 33.
- 37 M.D. Brodsky, N.J. Griffin and M.D. Odie, *J. Appl. Phys.*, **40** (1969) 895.
- 38 C.H. Chen and G.H. Lander, *Phys. Rev. Lett.*, **57** (1986) 110.
- 39 T.G. Berlincourt, *Phys. Rev.*, **114** (1959) 969.
- 40 C.A. Cornelius and T.F. Smith, *J. Low Temp. Phys.*, **40** (1980) 391.
- 41 C.A. Cornelius and T.F. Smith, *Solid State Commun.*, **38** (1981) 599.
- 42 D. Shoenberg, *Proc. Philos. Soc.*, **36** (1940) 84.
- 43 T.H. Geballe, B.T. Matthias, K. Andres, E.S. Fisher, T.F. Smith and W.H. Zachariasen, *Science*, **152** (1966) 755.
- 44 E.S. Fisher and D. Dever, *Solid State Commun.*, **8** (1970) 649.
- 45 T.F. Smith and E.S. Fisher, *J. Low Temp. Phys.*, **12** (1973) 631.